

AD 605711

**TECHNICAL INFORMATION SERIES**

**R64SD22**

**IONIZATION OF CESIUM AND SODIUM  
CONTAMINATED AIR IN THE HYPERSONIC  
SLENDER BODY BOUNDARY LAYER**

COPY	<u>2</u>	OF	<u>3</u>
HARD COPY	\$ . 2.00		
MICROFICHE	\$ . 0.50		

*36p*

**DDC**  
**RECEIVED**  
 SEP 24 1964  
**RESOLVED**  
 DDC-IRA C

**M. LENARD**

**SPACE SCIENCES  
LABORATORY**

# SPACE SCIENCES LABORATORY

IONIZATION OF CESIUM AND SODIUM CONTAMINATED AIR  
IN THE HYPERSONIC SLENDER BODY BOUNDARY LAYER

By

M. Lenard

R64SD22

August, 1964

MISSILE AND SPACE DIVISION

GENERAL  ELECTRIC

# CONTENTS

PAGE

Abstract	ii
INTRODUCTION	1
ANALYSIS	1
NUMERICAL RESULTS	13
DISCUSSION, CONCLUSIONS	19
ACKNOWLEDGMENTS	23
NOMENCLATURE	24
REFERENCES	26
APPENDIX	27

## ABSTRACT

An approximate procedure is used to predict the effect on air ionization of small amounts of cesium and sodium in the ablating surface material of pointed cones. Ionization is assumed to occur due to finite rate gas phase chemical reactions in the laminar boundary layer. An 11 species ( $N_2$ ,  $O_2$ , N, O, NO, Cs or Na,  $NO^+$ ,  $Cs^+$  or  $Na^+$ ,  $O_2^-$ ,  $O^-$ ,  $e^-$ ) 16 reaction chemical system is assumed.

## INTRODUCTION

For slender reentry bodies in hypersonic flight, the highest temperatures in the flow field may be attained in the boundary layer. Prediction of air ionization must then be based on solution of the boundary layer equations. Ionization in air is a complex process involving a large number of species and chemical reactions. For this reason, numerical computation procedures are necessary to make such predictions, particularly if the effect of finite chemical rates must be taken into consideration. Blottner<sup>1,2</sup> and others<sup>3</sup> have made such computations of ionization in hypersonic laminar boundary layers for pure air. The question arises whether some foreign species that contaminate the air in the boundary layer from an ablating or evaporating solid surface may not retard or promote the ionization process. Easily ionizable gases, such as alkali metal vapors, suggest themselves as "seeding" materials to promote the ionization process for various applications. The purpose of the present investigation is to predict the effects on air ionization of small amounts of cesium or sodium added to an ablating inert material that enters the boundary layer on pointed cones. As in other studies of boundary layers with complicated chemistry<sup>4</sup>, the effect of trace species on gross thermodynamic and fluid mechanic properties of the boundary layer is not considered. For simplicity it was assumed that the ablating inert material has the properties of air, thus neglecting any complicating effects of hydrocarbons on the ionization process.

## ANALYSIS

The laminar boundary layer equations on pointed cones are best written in transformed  $\eta, \xi$  coordinates<sup>2,5</sup>:

$$\xi = \int_0^x \rho_w \mu_w u_e r^2 dx$$
$$\eta = \frac{u_e r}{\sqrt{2\xi}} \int_0^y \rho dy \quad (1)$$

If velocity  $u$  is expressed as

$$u = u_e \frac{\partial f}{\partial \eta} \quad (2)$$

and the continuity equation is used to express  $v$  in terms of  $f$  the momentum and energy equations take on the following form:

Momentum:

$$\frac{\partial}{\partial \eta} \left( \iota \frac{\partial^2 f}{\partial \eta^2} \right) + f \frac{\partial^2 f}{\partial \eta^2} + \beta \left[ \frac{\rho_e}{\rho} - \left( \frac{\partial f}{\partial \eta} \right)^2 \right] = 2\xi \left[ \frac{\partial f}{\partial \eta} \frac{\partial^2 f}{\partial \eta \partial \xi} - \frac{\partial f}{\partial \xi} \frac{\partial^2 f}{\partial \eta^2} \right] \quad (3)$$

Energy:

$$\begin{aligned} & \frac{\partial}{\partial \eta} \left[ \frac{\iota}{Pr} \sum_{i=1}^7 c_i \frac{dh_i}{dT} \left( \frac{T_e}{h_e} \right) \frac{\partial}{\partial \eta} \left( \frac{T}{T_e} \right) \right] + f \sum_{i=1}^7 c_i \frac{\partial}{\partial \eta} \left( \frac{h_i}{h_e} \right) - \\ & \sum_{i=1}^7 \frac{\beta w_i}{\rho \frac{du_e}{dx}} \frac{h_i}{h_e} + \frac{u_e^2}{h_e} \left\{ \iota \left( \frac{\partial^2 f}{\partial \eta^2} \right)^2 + \right. \\ & \left. + \beta \frac{\partial f}{\partial \eta} \left[ \frac{T}{T_e} \left( \frac{\sum_{i=1}^7 c_i \frac{dh_i}{dT}}{\sum_{i=1}^7 c_{ie} \frac{dh_{ie}}{dT}} + \frac{2h_e}{\beta u_e^2} \sum_{i=1}^7 \frac{\partial c_{ie}}{\partial \ln \xi} \frac{h_{ie}}{h_e} \right) - \frac{\rho_e}{\rho} \right] \right\} - \\ & - \frac{\rho^2}{h_e \rho_w \mu_w} \frac{\partial T}{\partial \eta} \sum_{i=1}^7 \frac{q_i}{\eta_y} c_i \frac{dh_i}{dT} = 2\xi \sum_{i=1}^7 c_i \left\{ \frac{\partial f}{\partial \eta} \frac{\partial}{\partial \xi} \left( \frac{h_i}{h_e} \right) - \right. \\ & \left. - \frac{\partial f}{\partial \xi} \frac{\partial}{\partial \eta} \left( \frac{h_i}{h_e} \right) \right\} \quad (4) \end{aligned}$$

where

$$Pr \equiv \frac{\mu}{k} \sum_{i=1}^7 c_i \frac{dh_i}{dT} \quad (5)$$

$$l \equiv \frac{\rho \mu}{\rho_w \mu_w}$$

$$\beta \equiv \frac{2\xi}{u_e} \frac{du_e}{d\xi} = \frac{2\xi}{\rho_w \mu_w u_e^2 r^2} \frac{du_e}{dx} \quad (5) \text{ cont'd}$$

The species conservation equation is:

$$\begin{aligned} f \frac{\partial c_i}{\partial \eta} - \frac{1}{\rho_w \mu_w} \frac{\partial}{\partial \eta} \left( \rho^2 c_i \frac{q_i}{\eta_y} \right) + \frac{\beta}{\frac{du_e}{dx}} \left[ \frac{w_i}{\rho} - f \frac{c_i}{\eta c_{ie}} \left( \frac{w_i}{\rho} \right)_e \right] \\ = 2\xi \left[ \frac{\partial f}{\partial \eta} \frac{\partial c_i}{\partial \xi} - \frac{\partial f}{\partial \xi} \frac{\partial c_i}{\partial \eta} - \frac{\partial f}{\partial \eta} \frac{c_i}{c_{ie}} \frac{\partial c_{ie}}{\partial \xi} \right] \end{aligned} \quad (6)$$

where the flux velocities  $q_i$  are related to the gradients by equations of the type:

$$\sum_{j=1}^n \frac{M^2}{m_j} \frac{c_i c_j}{\delta_{ij}} \frac{q_j - q_i}{\eta_y} = \frac{\partial}{\partial \eta} M c_i \quad (7)$$

Plasma neutrality will be assumed due to the small Debye shielding distance at the conditions that are of practical interest. Thus, the diffusion of ions will be of the ambi-polar type and free diffusion of electrons need not be considered. However, the usual expressions for ambipolar diffusion must be modified due to the simultaneous presence of electrons and both positive and negative ions. For charged particles equation (7) is modified by the presence of a body force caused by a microscopic electric field due to local charge separation:

$$\sum_{j=1}^n \frac{M^2}{\delta_{ij}} \frac{c_i^{\pm} c_j}{m_i m_j} \frac{q_j - q_i^{\pm}}{\eta_y} = \frac{\partial}{\partial \eta} \left( \frac{M c_i^{\pm}}{m_i} \right)^{\pm} E \frac{c_i^{\pm}}{m_i} \quad (8)$$

Equation (8) is valid for all charged particles including electrons. For the assumed neutral plasma, the electron and ion concentrations and fluxes are related by charge concentration laws:

$$\frac{c_\epsilon}{m_\epsilon} = \sum_{i=1}^{n_p} \frac{c_i^+}{m_i} - \sum_{i=1}^{n_n} \frac{c_i^-}{m_i}$$

$$\frac{q_\epsilon c_\epsilon}{m_\epsilon} = \sum_{i=1}^{n_p} \frac{q_i^+ c_i^+}{m_i} - \sum_{i=1}^{n_n} \frac{q_i^- c_i^-}{m_i} \quad (9)$$

Equation (9) makes the electron diffusion equation (8) superfluous; the latter can then be used to eliminate electric field E from the remaining equations (8). The result is:

$$\sum_{j=1}^n \frac{M^2}{D_{ij}} \frac{c_i^\pm c_j}{m_i m_j} \frac{1}{\eta_y} \left[ q_j \left( 1 \pm \frac{D_{ij}}{D_{\epsilon j}} \right) - \left( q_i^\pm \pm \frac{D_{ij}}{D_{\epsilon j}} q_\epsilon \right) \right] =$$

$$= \frac{\partial}{\partial \eta} \left( \frac{M c_i^\pm}{m_i} \right) \pm \frac{c_i^\pm m_\epsilon}{c_\epsilon m_i} \frac{\partial}{\partial \eta} \left( \frac{M c_\epsilon}{m_\epsilon} \right) \quad (10)$$

where the total number of species n in (10) and subsequent equations does not include electrons. Due to the large mobility of electrons, the ratio  $D_{ij}/D_{\epsilon j}$  will be a small number;

$$\frac{D_{ij}}{D_{\epsilon j}} \approx \left( \frac{m_\epsilon}{m_i} \right)^{1/2} \approx 0.005 \ll 1.0 \quad (11)$$

Eliminating terms in (10) proportional to the small ratio in (11) one obtains the generalized ambipolar diffusion law for positive ions ;

$$\sum_{j=1}^n \frac{M^2}{\eta_y D_{ij}} \frac{c_i^+ c_j}{m_i m_j} (q_j - q_i^+) = \frac{\partial}{\partial \eta} \left( \frac{M c_i^+}{m_i} \right) + \frac{c_i^+ m_\epsilon}{c_\epsilon m_i} \frac{\partial}{\partial \eta} \left( \frac{M c_\epsilon}{m_\epsilon} \right) \quad (12)$$

For negative ions, the simplification of (10) is not so straightforward because the sum on the right hand side and the first sum on the left hand side will both be small, so that the small term involving  $q_\epsilon$  cannot any more be

considered insignificant compared to the remaining terms. Thus, for negative ions,

$$\begin{aligned} \sum_{j=1}^n \frac{M^2}{\eta_y \delta_{ij}} \frac{c_i^- c_j^-}{m_i m_j} \left( q_j^- - q_i^- + \frac{\delta_{ij}}{\delta_\epsilon} q_\epsilon \right) &= \\ &= \frac{\partial}{\partial \eta} \left( \frac{M c_i^-}{m_i} \right) - \frac{c_i^- m_\epsilon}{c_\epsilon m_i} \frac{\partial}{\partial \eta} \left( \frac{M c_\epsilon}{m_\epsilon} \right) \end{aligned} \quad (13)$$

A corollary of the foregoing development is that  $q_i^+$  is significantly larger than  $q_i^-$ . This fact can be utilized in conservation law (9), and the result substituted into (13);

$$\begin{aligned} \sum_{j=1}^n \frac{M^2}{\eta_y \delta_{ij}} \frac{c_i^- c_j^-}{m_i m_j} \left\{ q_j^- - q_i^- + \frac{\delta_{ij}}{\delta_{\epsilon j}} \sum_{k=1}^n \frac{c_k^+ m_\epsilon}{c_\epsilon m_j} q_k^+ \right\} &= \\ &= \frac{\partial}{\partial \eta} \left( \frac{M c_i^-}{m_i} \right) - \frac{c_i^- m_\epsilon}{c_\epsilon m_i} \frac{\partial}{\partial y} \left( \frac{M c_\epsilon}{m_\epsilon} \right) \end{aligned} \quad (14)$$

Equation (10) represents the most general form of ambipolar diffusion; it is based on the assumption of no macroscopic charge separation. Equations (12) and (14) are based on three additional assumptions:

- (a)  $\delta_{ij} \ll \delta_{\epsilon j}$  (eq. 11)
- (b)  $\delta_{ij} / \delta_{kl} \approx 1.0$  for all species except electrons
- (c)  $(c_i^- m_\epsilon / c_\epsilon m_i) \approx \text{constant}$

These assumptions are reasonable for chemi-ionization in the boundary layer where all species in the mixture have similar molecular weights.

If the further simplification of a "constant Lewis number" is made, i. e.:

$$\delta_{ij} = \delta, \quad \delta_{\epsilon j} = \delta_\epsilon \quad (15)$$

equations (7), (12) and (14) reduce to:

$$\begin{aligned}
\frac{M}{\eta_y} \frac{c_i q_i}{m_i} &= - \delta \frac{\partial}{\partial \eta} \left( \frac{Mc_i}{m_i} \right) \\
\frac{M}{\eta_y} \frac{c_i^+ q_i^+}{m_i} &= - \delta \left[ \frac{\partial}{\partial \eta} \left( \frac{Mc_i^+}{m_i} \right) + \frac{c_i^+ m_\epsilon}{c_\epsilon m_i} \frac{\partial}{\partial \eta} \left( \frac{Mc_\epsilon}{m_\epsilon} \right) \right] \\
\frac{M}{\partial y} \frac{c_i^- q_i^-}{m_i} &= - \delta \left\{ \frac{\partial}{\partial y} \left( \frac{Mc_i^-}{m_i} \right) - \frac{c_i^- m_\epsilon}{c_\epsilon m_i} \left[ \frac{\partial}{\partial \eta} \left( \frac{Mc_\epsilon}{m_\epsilon} \right) - \right. \right. \\
&\quad \left. \left. - \frac{\delta}{\epsilon} \sum_{k=1}^{n_p} \left\{ \frac{\partial}{\partial \eta} \left( \frac{Mc_k^+}{m_k} \right) + \frac{c_k^+ m_\epsilon}{c_\epsilon m_k} \frac{\partial}{\partial \eta} \left( \frac{Mc_\epsilon}{m_\epsilon} \right) \right\} \right] \right\} \quad (16)
\end{aligned}$$

Results (16), together with (9), represent the generalizations of Fick's law in the boundary layer for ambipolar diffusion in a many-ion mixture.

Thermodynamic and chemical kinetic relationships are required to complete the system of equations:

$$\begin{aligned}
\frac{p}{R} &= \frac{\rho T}{M} = \text{constant} \\
\frac{i}{M} &= \sum_{i=1}^n \frac{c_i}{m_i} \\
h_j &= h_j(T) \\
w_i &= w_i(\rho, T, c_j) \quad (17)
\end{aligned}$$

Except for the role of negative ions, the foregoing system of equations is derived and discussed in detail in reference 5; numerical results for the pure air system are given in references 1, 2 and 5; details of thermodynamic transport and chemical properties that were employed are given in reference 5. It is noteworthy that for a pointed cone there was no substantial difference between numerical results of reacting and ionizing air boundary layer obtained for the general non-similar case by an exact implicit finite difference scheme<sup>1</sup>, or the so-called locally similar solution<sup>5</sup>, which neglects all derivatives with respect to  $\xi$ .

The physico-chemical processes that take place in the laminar hypersonic boundary layer on cones can be ascertained both from the species conservation equation (6) and the numerical results obtained for pure air. The quantity  $\beta (du_e/dx)^{-1}$  that determines how large the chemical mass generation rate terms are in the differential equation, increases from 0 at the tip of the cone to large values far downstream. Correspondingly, the numerical results in references 1, 2, and 5 indicate that near the tip the boundary layer composition is essentially frozen, and as distance increases, and the boundary layer thickness grows, a gradual relaxation towards equilibrium composition in the boundary layer takes place. The principal chemical activity occurs in a narrow high temperature region of the boundary layer from where the reaction products diffuse towards the catalytic wall surface and towards the free stream. For a reasonably cold wall surface and for slender cones where the inviscid flow temperature is low, the concentrations of the reaction products at a catalytic wall and in the free stream will both be insignificant. This makes it possible to introduce the assumption of "similar" composition profiles for all reaction products in the boundary layer by means of a function of  $\eta$  and  $\xi$ , i. e.:

$$c_i(\eta, \xi) = c_{i \max} F(\eta, \xi) \quad (18)$$

for all  $c_i$  that are reaction products. Function  $F$  has the desired properties of vanishing at the wall and far from the wall and rising to a sharp peak in the high temperature region. Assumption (18) is the basis of the present investigation of estimating the effect of small amounts of cesium or sodium in the ablating inert material of the cone surface.

Let three assumptions now be made to simplify the description of the inter-diffusion of chemical species in the boundary layer:

- (a) All binary diffusion coefficients are equal at a given temperature
- (b) For the purposes of diffusion laws all species have the same molecular weights.
- (c) The resulting Schmidt number is a constant regardless of temperature.

Subject to the above assumptions, Fick's law is recovered, and the species conservation equations (6) and diffusion equations (6) for neutral species can be combined:

$$f \frac{\partial c_i}{\partial \eta} + \frac{1}{Sc} \left( \nu \frac{\partial c_i}{\partial \eta} \right) + \frac{\beta}{\frac{du_e}{dx}} \frac{w_i}{\rho} = 2\xi \left[ \frac{\partial f}{\partial \eta} \frac{\partial c_i}{\partial \xi} - \frac{\partial f}{\partial \xi} \frac{\partial c_i}{\partial \eta} \right] \quad (19)$$

The total mass fraction of constituent elements in the boundary layer can be related to the mass fraction of the individual species:

$$c^j = \sum_{i=1}^n \frac{m^j}{m_i} \alpha_i^j c_i \quad (20)$$

where  $\alpha_i^j$  is the number of atoms of elements  $j$  in species  $i$ , and the  $m$  -  $s$  are the respective molecular (or atomic) weights. Since elements are conserved in a chemical reaction, i. e.:

$$\sum_{i=1}^n \frac{m^j}{m_i} \alpha_i^j w_i = 0 \quad (21)$$

an equation for conservation of elements may be written by neglecting trace amounts of ionized species and by applying summation (20) to equations (19):

$$f \frac{\partial c^j}{\partial \eta} + \frac{1}{Sc} \frac{\partial}{\partial \eta} \left( \nu \frac{\partial c^j}{\partial \eta} \right) = 2\xi \left[ \frac{\partial f}{\partial \eta} \frac{\partial c^j}{\partial \xi} - \frac{\partial f}{\partial \xi} \frac{\partial c^j}{\partial \eta} \right] \quad (22)$$

For pointed cones  $\beta = 0$ , so that comparison of (3) and (22) reveals that a "Reynolds analogy" can be established for the element concentrations by a simple transformation which incorporates the Schmidt number into the coordinate  $\eta$  ;

$$\frac{c^j(\eta, \xi) - c^j(0, \xi)}{c_e^j - c^j(0, \xi)} = \frac{\partial f}{\partial \eta}(Sc \eta, \xi) \quad (23)$$

provided elemental concentration  $c^j(0, \xi)$  is independent of  $\xi$  or "local" similarity is assumed. (It will be shown below that for realistic injection rate distribution the latter assumption is necessary.) What the concentrations of various elements are at the wall remains to be determined from the

boundary conditions. The general boundary conditions for species diffusing to and from a catalytic wall where material is injected are:

$$v_w \left[ c_w^j - c^j(0, x) \right] = \sum_{i=1}^n \frac{m_i}{m_i} \alpha_i^j c_i q_i \Big|_{y=0} \quad (24)$$

where  $v_w$  is an injection velocity corresponding to the mass injection rate and density on the wall surface; and  $c_w^j$  the mass fraction of the  $j$ -th element in the injected gas. Boundary condition (24) accounts for the fact that the total amount of element  $j$  in the species diffusing to and from the wall changes due to the enrichment by the gas that is ejected from the surface ( $c_w^j$ ) as it mixes with the boundary layer fluid ( $c^j(0, x)$ ). Using the transformed coordinate system and the approximations implicit in (16), boundary condition (24) can be rewritten:

$$\sqrt{2\xi} \frac{v_w}{\nu u_e} \left[ c_w^j - c^j(0, \xi) \right] = \left( \frac{d\eta}{dy} \right)^{-1} \rho \sum_{i=1}^n \frac{m_i^j}{m_i} \alpha_i^j c_i q_i = - \frac{\mu}{Sc} \frac{\partial c^j}{\partial \eta} \Big|_{\eta=0} \quad (25)$$

Using (23) in conjunction with (25) one may solve for the elemental composition at the wall:

$$c^j(0, \xi) = \frac{x^{1/2} c_w^j + I c_e^j}{x^{1/2} + I} \quad (26)$$

where  $I$  is the injection parameter;

$$\frac{I}{x^{1/2}} = \frac{\mu(0) r}{(2\xi)^{1/2} v_w} \frac{\partial u}{\partial \eta} \Big|_{\eta=0} = \left( \frac{3\mu(0)}{2\rho(0) u_e x} \right)^{1/2} \frac{1}{v_w} \frac{\partial u}{\partial \eta} \Big|_{\eta=0} \quad (27)$$

and the second form of  $I$  in (27) is based on constant wall and free stream properties for a cone. It can be seen from (26) and (27) that, except for special conditions,  $c^j(0, \xi)$  will be a function of  $\xi$ . Expression (23) must then be justified by the assumption of local similarity. As mentioned before, for pure air this assumption was found reasonably valid<sup>5</sup>, and, unless there are sudden variations of  $c_w^j$  and  $I$  along the body, it still appears reasonable for contaminated air.

Now finally the problem of injecting an inert gas containing small amounts of cesium or sodium can be considered. Let the injected inert gas have the properties of air, and let the amount of cesium or sodium be sufficiently small so that the gross thermal and fluid mechanic properties of the flow remain unchanged by the addition. The air chemistry<sup>7</sup> used in reference 1, 2 and 5 can then be used to calculate properties of the boundary layer with air injection for a given flight condition. This system considers  $\text{NO}^+$  as the sole source of ionized particles. Let the total cesium or sodium concentration be determined by (26) and (23). Furthermore, let the additional ionization products due to the presence of cesium be related to the  $\text{NO}^+$  ions by the "similarity law" of equation (18). Differential equation (19) can now be considered for the ionization products at the point where the ion concentrations are the maximum (i. e.  $\partial F / \partial \eta = 0$ ). Corresponding to equations (16) different expressions are obtained for the positive and negative ions respectively:

$$\left\{ \frac{2\ell}{Sc} \frac{\partial^2 F}{\partial \eta^2} c_{i \max}^+ + \left( \beta / \frac{du_e}{dx} \right) \frac{w_i^+}{\rho} \right\}_{\eta = \eta_{\max}} = 0$$

$$\left\{ \frac{2\ell}{Sc} \frac{\partial^2 F}{\partial \eta^2} \frac{\partial}{\partial \epsilon} \left( \sum_{k=1}^n \frac{c_{k \max}^+ m_\epsilon}{c_\epsilon m_k} \right) c_{i \max}^- + \left( \beta / \frac{du_e}{dx} \right) \frac{w_i^-}{\rho} \right\}_{\eta = \eta_{\max}} = 0$$

(28)

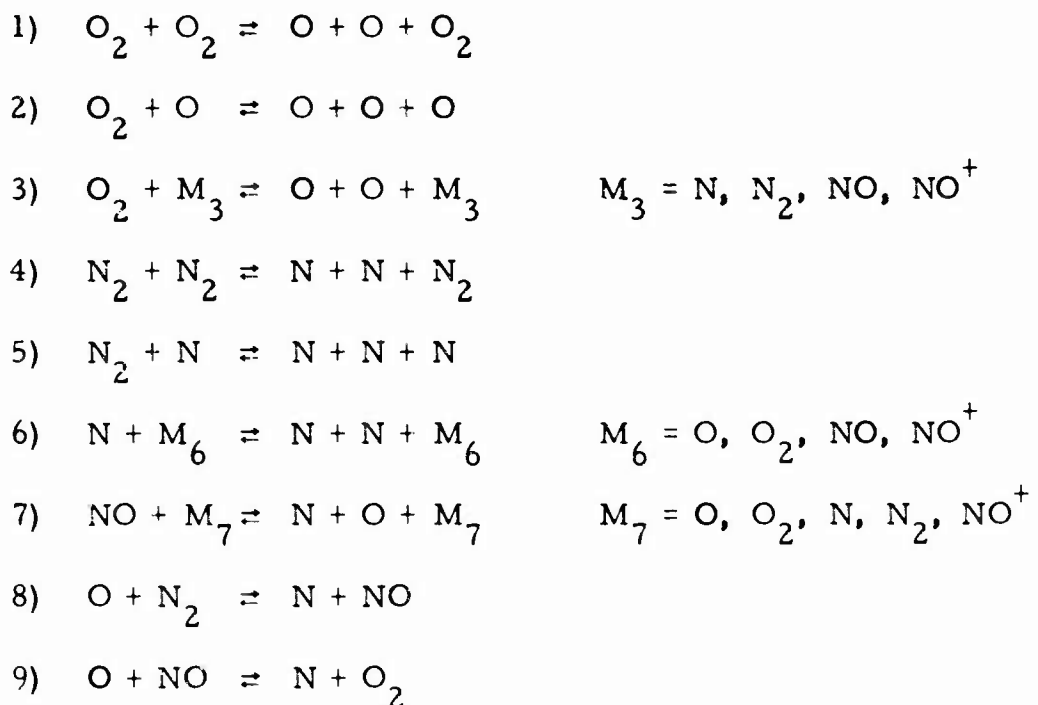
where  $\eta_{\max}$  denotes the location of the peak temperature and reaction products in the boundary layer, and the assumption of local similarity eliminates terms on the right hand side of the differential equation. In accordance with statement (18) pure air solutions (e.g., references 1, 2, 3, and 5) can be used to determine properties of function F:

$$-K \equiv \left. \frac{\partial^2 F}{\partial \eta^2} \right|_{\eta_{\max}} = \left. \frac{\partial^2 c_{\text{NO}^+}}{\partial \eta^2} \right|_{\eta_{\max}} / c_{\text{NO}^+ \max} \quad (29)$$

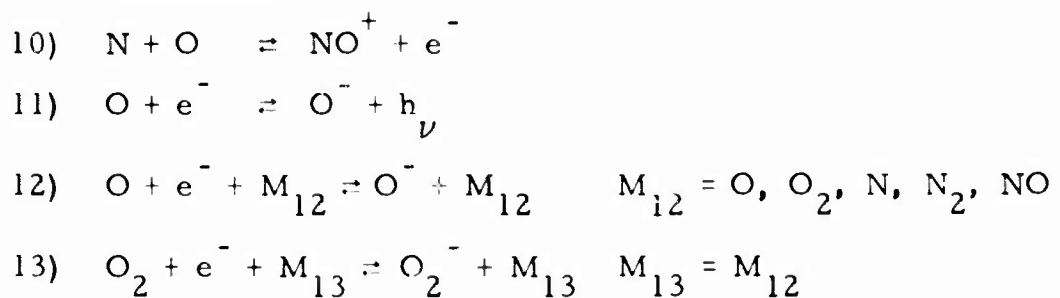
so that for a given ionization chemistry (28) represent a system of non-linear algebraic equations for the unknown peak concentrations of the ionization products,  $c_{i_{\max}}$ , in the boundary layer. The thermodynamic properties, velocities, concentration of major (non-ionized) species are assumed to remain unchanged from the numerical solution obtained for pure air injection. The total contaminant content at  $\eta_{\max}$  is known as a function of injection parameter I and the contaminants concentration in the surface material  $c_w^j$ . To complete description of the problem, the ionization chemistry of the cesium-air and sodium-air systems must now be described.

The system of chemical reactions that was considered is given below:

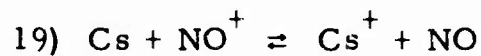
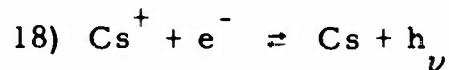
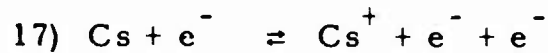
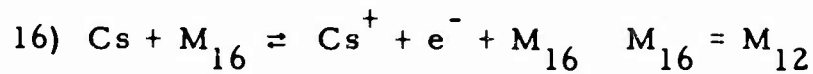
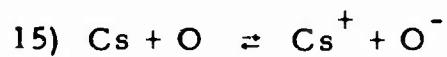
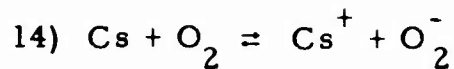
Non-ionizing air reactions:



Pure air ionization



The air-cesium and air-sodium ionization reaction systems are identical differing only in their rate constants, e.g. for air cesium ionization:



The rate constants for reactions 1 through 10 are given in Bortner's<sup>7</sup> report; they are identical to the chemical system used in references 1, 2 and 5. For reactions 11 and 12, and the sodium system (reactions 14 through 19) Bortner's<sup>8</sup> latest rate constants were used. Reaction 13 was assumed to be in equilibrium, the corresponding equilibrium constant, and the rate constants for the cesium system (reactions 14 through 19), are based on Browne and Schwartz's<sup>6</sup> work. These rate constants are all listed in Appendix I, including additional, and unrealistically slow, rate constants for reaction 12. These "slow" rates were used to explore the potential significance of increased  $\text{O}^-$  concentrations on the ionization process. It may be observed that the five unknown charged particle concentrations can be reduced to a system of three unknowns by the use of overall charge conservation and the partial equilibrium of reaction 13. The solution of the ionization problem then reduces to solving non-linear algebraic system (28) for three charged particle concentrations, arbitrarily chosen as  $\text{Cs}^+$  or  $\text{Na}^+$ ,  $\text{NO}^+$ , and  $\text{O}^-$ . The result will be a function of distance along the body, the thermo-chemical state of the uncontaminated air at the peak temperature point in the boundary layer, and the total contaminant content at that point. The latter depends on the various factors that are determined by the injection process.

## NUMERICAL RESULTS

Numerical solutions of equations (28) were obtained for conditions summarized in Table I.

TABLE I  
PRINCIPAL FLIGHT CONDITIONS

<u>Cone half angle</u>	<u>Altitude k ft.</u>	<u><math>u_{\infty}</math> k ft./sec</u>	<u><math>u_e</math> k ft./sec</u>	<u><math>\rho_e</math> <math>10^{-3}</math> atm</u>	<u><math>T_w</math> <math>^{\circ}</math>K</u>	<u>Contaminant</u>
$10^{\circ}$	150	22	21.59	27.56	1000	Cs
$10^{\circ}$	200	22	21.59	4.6706	1000	Cs
$10^{\circ}$	150	22	21.59	27.56	1000	Na
$10^{\circ}$	75	20.72	20.334	747.61	1555.6	Na
$9.03^{\circ}$	150	24.5	24.129	27.616	1450	Na

The distances,  $x$ , from the tip of the cone ranged from 0.1 to 10 ft. In addition to the principal flight conditions several "hybrid" conditions were also investigated in order to determine the effect of changing only one of the variables (i. e. density, temperature, etc.) on the solution. It was found that the greatly reduced diffusivity of the negative ions had no significant effect in reducing peak electron densities, except for the more slowly ionizing sodium case, and only for artificially reduced rates of the  $O^-$  detachment reaction (reaction 12). For this reason, the special properties of the negative ions were neglected in the majority of the calculations. Table II presents a summary of the principal results. Since the foregoing treatment of the ionization problem is completely separate and distinct from the injection process, Table II is presented in terms of the total contaminant content at the peak temperature point ( $C^{Cs}(\eta_{\max})$  or  $C^{Na}(\eta_{\max})$ ), which quantity in turn depends on the injection parameters (equations 23 and 26).

TABLE II

## IONIZATION AT THE PEAK TEMPERATURE POINT IN THE BOUNDARY LAYER

H	Ue	x	T	$\rho$	$c_{O_2}$	$c_C$	$c_N$	$c_{Cs,Na}$	$N_{Cs,Na}^+$	$N_e^-$	$N_{NO}^+$	$N_{NO}^-$	Cs, Na
kft	kft/sec	ft	$^{\circ}K$	$10^{-6}$ g/cc	$10^{-3}$	$10^{-5}$	$10^{-5}$	$10^{-6}$	$\times 10^{10}$	particles/cc			% ionized
Cesium													
150	21.59	4.5	4607	2.101	.2307	1.71	.3008	.0409	.03523	.03528	.00006	.00001	90.6
150	21.59	4.5	4607	2.101	.2307	1.71	.3008	40.9	35.26	35.26	.00006	.00	90.6
"Hybrid"	21.59	4.5	4607	.3561	.2307	1.71	.3008	.0409	.004079	.004078	.000002	.000003	61.8
"	21.59	4.5	4607	.3561	.2307	1.71	.3008	40.9	4.099	4.096	.000002	.003	62.1
"	21.59	4.5	4569	2.118	.232	.328	.03778	40.9	35.27	35.27	0	0	89.9
"	21.59	.45	4569	2.118	.232	.328	.03778	40.9	18.47	18.47	"	0	47.05
"	21.59	.045	4569	2.118	.232	.328	.03778	40.9	3.186	3.181	"	.005	8.12
"	21.59	4.5	4569	35.9	.232	.328	.03778	40.9	660.7	660.7	"	0	99.5
"	21.59	.45	4569	35.9	.232	.328	.03778	40.9	673.7	623.7	"	0	93.8
"	21.59	.045	4569	35.9	.232	.328	.03778	40.9	400.6	400.5	"	0.1	60.25
200	21.59	4.5	4569	.359	.232	.328	.03778	40.9	4.006	4.05	"	.001	60.25
200	21.59	.45	4569	.359	.232	.328	.03778	40.9	.8665	.8656	"	.0009	13.04
200	21.59	.045	4569	.359	.232	.328	.03778	40.9	.09806	.09775	"	.00031	1.475
Sodium													
150	21.59	0.1	4613	2.098	.2327	.0326	.000974	3.243	.001351	.001350	0	.000001	.00758
150	21.59	0.3	4612	2.099	.2326	.126	.001124	5.442	.006857	.006850	"	.000007	.0229
150	21.59	1.0	4609	2.100	.2323	.424	.0583	9.367	.04033	.04029	"	.00004	.0783
150	21.59	3.0	4600	2.104	.2312	1.25	.214	14.85	.2044	.2042	"	.0002	.250
150	21.59	3.0	4600	2.104	.2312	1.25	.214	14.85	.002044	.002063	.000021	.000002	.250
150	21.59	9.9	4572	2.117	.2285	3.855	.734	23.18	1.240	1.240	.001	.001	.965
150	24.129	0.1	5699	1.702	.2321	.287	.0589	2.268	.005400	.005388	0	.000012	.0534
150	24.129	0.3	5685	1.702	.2314	.846	.261	3.843	.02777	.02771	"	.00006	.162
150	24.129	1.02	5650	1.702	.2286	2.783	1.205	6.788	.1758	.1756	.0002	.0004	.581
"Hybrid"	24.129	1.02	5650	1.702	.2286	.02783	1.205	6.788	.1461	.1461	0	0	.483
150	24.129	3.02	5560	1.702	.2213	7.562	3.902	10.96	.9101	.9140	.0054	.0015	1.864
75	20.334	3.05	4167	63.01	.2086	12.31	1.833	1100	9872	9870	1	3	5.437
75	20.334	3.05	4167	63.01	.2086	12.31	1.833	11	98.68	9940	.75	.03	5.435
75	20.334	3.05	4167	63.01	.2086	12.31	1.833	0.11	.9868	1.7346	.7481	.0003	5.435
"Hybrid"	20.334	3.05	4167	630.1	.2086	12.31	1.833	1100	652000	652000	75	27	35.9
"	20.334	3.05	4167	630.1	.2086	12.31	1.833	11	6627	6702	75	0	36.5
"	20.334	3.05	4167	630.1	.2086	12.31	1.833	0.11	66.27	141.08	74.81	0	36.5

Examination of the results of Table II indicated that only the forward ionization rates of the contaminant were significant in determining the fraction of contaminant that was ionized. The non-linear system (28) can then be greatly simplified to get an explicit solution for the fraction of sodium or cesium that is ionized at the peak temperature point:

$$\frac{c_{\text{Na}}^+}{c_{\text{Na}}(\eta_{\text{max}})} = \left[ 1.0 + \frac{3 l K u_e}{S c \rho x \left( \frac{k_{14} c_{\text{O}_2}}{32} + \frac{k_{15} c_{\text{O}}}{16} + \frac{k_{16}}{m} \right)} \right]^{-1.0} \quad (30)$$

Equation (30) was found to represent the % of contaminant ionized (Table III) within 5%. Discrepancies arose only at the highest densities of charged contaminant particles, where the loss due reaction 18 amounted to a few percent. Reaction 15 was found to be the most rapid, but due to the small concentrations of O, reaction (14) often dominated the result. The effect of O concentration is shown explicitly in one of the cases in Table II where  $C_{\text{O}}$  was changed from .278 to .00278%. It is expected that for conditions where the electron densities are significantly larger than for the cases presented in Table II reaction 17 (ionization of contaminant by collision with electrons) may also have to be considered. In that case, the simple formula (30) may have to be modified.

Table II also shows the close relationship between the particle densities of electrons and contaminant ions; differences were due to the presence of three other charged particles;  $\text{NO}^+$ ,  $\text{O}^-$  and  $\text{O}_2^-$ . For all cases that were considered, the presence of  $\text{O}_2^-$  did not influence electron density to the four significant figures that are presented in Table II. Only for the cases where the total contaminant concentrations were very small did the presence of  $\text{NO}^+$  ions add significantly to the peak electron density. It is noteworthy that there was no effective coupling between the production of  $\text{NO}^+$  ions and the ionization of the contaminant. The reason for this is that the reactions involving charged-neutral collisions, which may have coupled the two types of ionization processes,

occurred much less frequently than the ion producing neutral-neutral collisions. The only detectable change in  $\text{NO}^+$  production from the pure air case was due to a slight depletion of the  $\text{NO}^+$  producing oxygen atom supply due to the presence of  $\text{O}^-$ .

Equation (28) and (11) imply that in a neutral plasma diffusion of the  $\text{O}^-$  (and other negative) ions may be reduced by as much as two orders of magnitude. This retardation of the diffusion is due to the microscopic electric field created by the tendency of electrons to "escape", the resulting electrically attracting region then hampers diffusion of the larger negative particles. In the ionizing boundary layer this retarded diffusion may cause an "accumulation" of  $\text{O}^-$  (or other negative) ions in the reaction zone, greatly reducing thereby the electron densities in the flow. The importance of this effect was investigated by comparing calculations where the retarded diffusivity of  $\text{O}^-$  was not accounted for with the more exact result. An unrealistically slow reaction rate for  $\text{O}^-$  detachment was also compared to the exact result. The results of these comparisons are shown in Table III. The examples for this comparison were taken from Table II for sodium contamination; a  $9:03^\circ$  cone flying at 24,500 fps and a  $10^\circ$  cone flying at 22,000 fps, both at 150,000 ft. altitude were considered.

TABLE III

EFFECT OF  $\text{O}^-$  ON PEAK ELECTRON DENSITIES ( $x = 3.0$  ft)

$U_x$ fps, $T_{\text{max}}^\circ\text{K}$	24500 fps, 5560 $^\circ\text{K}$				22000 fps, 4600 $^\circ\text{K}$			
$\text{O}^-$ Diffusion Law	exact	same as +	exact	same as +	exact	same as +	exact	same as +
Reaction 12 rates	reg.	reg.	slow	slow	reg.	reg.	slow	slow
$c_{\text{Na}}(\eta_{\text{max}})$	← .1096 x 10 <sup>-4</sup> →				← .1485 x 10 <sup>-4</sup> →			
% Na ionized	← 1.864 →				← .2500 →			
$N_{\text{Na}}^+$	← .9101 →				← .2044 →			
$N_{\text{NO}}^+$	← .0054 →				← 0 →			
$\left. \begin{matrix} N_{\text{O}}^- \\ N_e^- \end{matrix} \right\} \frac{10^{10} \text{ particles}}{\text{cc}}$	.0016	.0015	.8544	.2378	.0002	.0002	.1160	.0215
	.9130	.9140	.0611	.6777	.2042	.2042	.0885	.1830

The results of Table III show that the detachment of electrons from  $O^-$  is so rapid that the slow diffusion rates have no effect on the outcome of the calculations. At the "slow" detachment rates the outcome is quite different, the accumulation of  $O^-$  significantly reduced peak electron densities in the boundary layer. This indicates that it may be important for some types of negative ions to calculate the details of the diffusion process in reacting laminar boundary layers in order to predict ionization accurately. This is not necessary for  $O^-$  because of the rapid disappearance of this ion due to electron detachment which counteracts the  $O^-$  production of the ionizing contaminant. For the conditions that were considered, reactions 15 (forward) and 12 (reverse) were the only two reactions that affected production of  $O^-$ , so that it was possible to solve equation (28) explicitly for the peak  $O^-$  concentration:

$$c_{O^-}^{\max} = \frac{k_{15} c_O (c_{Na}/23)}{(k'_{12}/M) + (.015 l K u_e / Sc \rho x)} \Bigg|_{\eta = \eta_{\max}} \quad (31)$$

where electron and positive particle concentrations were assumed approximately equal, so that;

$$\frac{S}{D_\epsilon} \left( \sum_{k=i}^{n_p} \frac{c_{k \max}^+ m_\epsilon}{c_{\epsilon \max} m_k} \right) \cong 0.005 \quad (32)$$

Equation (30) and the sodium (cesium) conservation law can be used to rewrite (31);

$$\frac{c_{O^-}^{\max}}{c_O(\eta_{\max}) c_{Na}(\eta_{\max})} = \frac{G_1 \rho x}{(G_1 + \rho x) (G_2 + \beta \rho x)} \quad (33)$$

where;

$$\begin{aligned}
G_1 &\equiv \frac{3 \ell K u_e}{Sc \left[ \frac{k_{14} c_{O_2}}{32} + \frac{k_{15} c_O}{16} + \frac{k_{16}}{M} \right]} \\
G_2 &\equiv \frac{.015 \ell K u_e}{Sc (k_{15}/23)} \\
G_3 &\equiv \frac{k'_{12} 23}{k_{15} M}
\end{aligned} \tag{34}$$

Result (33) reaches a peak value when;

$$\rho_x = \left( \frac{G_1 G_2}{G_3} \right)^{1/2} \tag{35}$$

at which point;

$$\frac{c_{O^-}(\eta_{max})}{c_{O^-}(\eta_{max}) c_{Na^+}(\eta_{max})} = \frac{G_1}{2(G_1 G_2 G_3)^{1/2} + G_1 G_3 + G_2} \tag{36}$$

It can be seen that when  $G_3$  is very large (fast electron detachment from  $O^-$ ) the value of  $G_2$  is immaterial, because the  $O^-$  concentration will always be small, approaching  $1/G_3$  in the limit. Physically, this means that in this limiting case the concentration of  $O^-$  is determined by an "equilibrium" between the production of  $O^-$  by reaction 15 forward and the consumption of  $O^-$  by reaction 12 in reverse; diffusion plays no role. For  $G_3$  not large, a small  $G_2$  (reduced diffusivity) will increase the peak concentrations of the negative ions greatly. This explains the results of Table III.

## DISCUSSION, CONCLUSIONS

The applicability of the approximate method that has been used in the foregoing calculations is limited by the underlying assumptions. These include the requirement that all reaction products originate in the high temperature region of the boundary layer, that the wall be catalytic, and that the boundary conditions change slowly if at all, to insure local similarity. The latter implies that if the body is not a slender cone it must be a pointed slender body with slowly varying surface slope. The accuracy of the method is further limited by the fact that due to the differences between the chemical and transport properties of the different species the maxima in temperature and the various reaction products do not exactly coincide, and that the correlation factor  $K$  (eq. 29) varies from species to species. For  $\text{NO}^+$  and Blottner's pure air cases (ref. 1)  $K$  was found to vary between 3.1 and 3.5. (This was also true of the other, non-ionized reaction products with the exception of  $\text{N}$ .) For the cesium calculations (Table II.),  $K$  was taken as 3.43, for the sodium cases (which varied over a wider range of conditions) a value of  $K = 3.3$  was used,  $\ell$  being .63 and  $\text{Sc} = .5$  in both cases. For large injection rates, the thickening of the boundary layer will make  $K$  smaller. Examination of a few preliminary numerical boundary layer solutions (Blottner, ref. 1) with injection suggests that

$$K = \frac{K(\text{no injection})}{\eta_{\max}} \cong \frac{3.3}{\eta_{\max}} \quad (37)$$

may adequately describe this effect. Locally similar solutions with injection have been examined resulting in a relation:

$$\eta_{\max} = 1.0 + \frac{11.5}{(I)^2} \times (\text{ft.}) \quad (38)$$

that may be useful. Relations (37) and (38) have not been used in the foregoing results, and must be considered conjectural. They may however form the basis, together with equation (30), of correlating results of exact numerical

calculations, as they become available. It is expected that  $K$  will also be a weak function of pressure, wall temperature, maximum temperature, and other parameters of the problem. In particular, as the ionization approaches 100% and equilibrium is approached the shape of the profiles will certainly change toward a  $K$  decreased severalfold, and the peak ion contaminant concentration will shift its location toward the wall. The present method is then not well suited to conditions near ionization equilibrium.

The treatment of the contaminant injection in the foregoing simplified analysis is entirely separate from the ionization problem. It is based on constant (or slowly varying) injection velocity and contaminant content in the ablating material. If these assumptions are not true, but the total contaminant content at the peak temperature point can be calculated or estimated by some other method, the calculation of the ionization can still proceed by means of equations (28). For most of the results that were calculated

$$\frac{u}{u_e} (Sc \eta_{\max}) = 0.24$$

$$\frac{1}{u_e} \left. \frac{\partial U}{\partial \eta} \right|_{\eta=0} = 0.40 \quad (39)$$

represent reasonable approximations.

Finally, comparison of the approximate method with a preliminary exact result, heretofore unpublished, was made possible thanks to the courtesy of the author's colleague Dr. F. G. Blottner. Injection of sodium contaminated air was considered for a simplified chemical system consisting of reaction 1 through 12 and 15. (The approximate results were also computed for this simplified chemical system; i.e. reactions 10 through 12 and 15.) The conditions of the comparison and the results are summarized in Table IV.

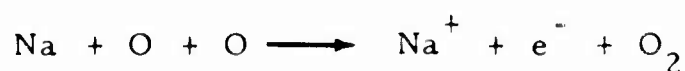
TABLE IV.

COMPARISON OF EXACT AND APPROXIMATE SOLUTIONS

Input		Results at $\eta_{max}$		
			Exact	Approximate
Cone angle	$10^\circ$			
Altitude	150,000 ft			
$u_\infty$	22,000 fps	$C^{Na} \times 10^5$	1.362	1.361
$u_e$	21,570 fps			
$T_e$	$1,000^\circ K$			
$T_w$	$4,478^\circ K$	$N_{Na}^+$	45.70	40.28
$T_{max}$		$N_{Na}^+$		
$\rho_l(\eta_{max})$	$.2161 \times 10^{-5} \text{ g/cc}$			
$l$	.62845	$N_{NO}^+$	.5165	.4164
K	3.1273			
I	4.5809	$N_{O}^-$	.0976	.1097
$C_{O_2}$	.206	$N_{O}^-$		
$C_{CO}$	$.33555 \times 10^{-3}$			
$C_{Na}$	$1.0 \times 10^{-4}$	$N_e^-$	46.12	40.59
$x$	1.2 ft			

The agreement for  $C^{Na}$  up to the fourth significant figure must be considered fortuitous. The remaining results however agree within the expected accuracy of the thermochemical properties of the reacting gas.

At the conclusion of this work Kane's<sup>9</sup> report for sodium contaminated air ionization came to the author's attention. In comparison with the present work, Kane<sup>9</sup> makes the same series of fluid mechanic assumptions. His treatment of the injection is identical except for a more complicated form of the "Reynolds analogy". The solution of the equation is performed by numerically evaluating integrals over the entire boundary layer (Kane<sup>9</sup> did not take advantage of the short cut afforded by equations (28) of the present report). Finally, Kane's kinetics for sodium are taken from Bortner's earlier work, which has been superseded since. (The complicating effects of  $O_2^-$ ,  $O^-$  are not accounted for by Kane<sup>9</sup>, this may not result in serious error.) In particular, the reaction that dominates Kane's<sup>9</sup> results



should be replaced by reaction 14 and 15. Finally, Kane<sup>9</sup> does not account for the effect of depletion of the contaminant material on the ionization rate. Thus, Kane's<sup>9</sup> equation (36) gives a linear growth law for  $N_{Na}^+$  vs  $x$ , which is equivalent to expanding equation (30) of the present analysis in powers of  $x$ . The more accurate expression, eq. (30), is superior when the fraction of contaminant ionized becomes significant.

In conclusion, it can be stated that, subject to the assumptions of the analysis:

(1) The approximate method gives reasonable predictions of the non-equilibrium ionization process in contaminated laminar hypersonic boundary layers on slender bodies.

(2) The injection and ionization processes are independent.

(3) The ionizations of pure air and the alkali metal contaminant are decoupled.

(4) The ionization of alkali metal contaminants in laminar hypersonic slender body boundary layers is dominated by the forward ionization rates and can be expressed by a simple formula (eq. 30), unless contaminant ionization due to electron-contaminant collision (reaction 7) becomes important.

(5) Due to the high detachment rate of electrons from  $O^-$ , the presence of these ions does not affect the result significantly in spite of their retarded diffusion rates.

(6) The results of this approximate method can be used to make predictions of contaminant ionization and to correlate and explain results of exact calculations as they become available.

## ACKNOWLEDGEMENTS

The use of some heretofore unpublished results of numerical calculations of contaminated boundary layers is gratefully acknowledged to Dr. F. G. Blottner. The numerical work presented in this report was ably performed by Mrs. E. Dean.

## NOMENCLATURE

$c_i$	Mass fraction of i-th species
$c^i$	Mass fraction of i-th element
$D_{ij}$	Mixture diffusion coefficient
$D_{ij}$	Binary diffusion coefficient
$E$	Body force due to microscopic electric field
$f$	Nor.-dimensional stream function (Equation 2)
$F$	Similarity function (Equation 18)
$G_1, G_2, G_3$	Equation (34)
$h$	Mixture enthalpy
$h_i$	Species enthalpy
$I$	Injection parameter (Equation 27)
$k$	Mixture (frozen) heat conductivity
$k_{11}, k_{12}$	Chemical rate constants for 11-th, 12-th etc. reaction
$K$	$K = -\partial^2 F / \partial y^2 \Big _{\eta = \eta_{\max}}$ (Equation 29)
$\rho$	Density-viscosity product (Equation 5)
$m_i$	Molecular weight of i-th species
$M$	Molecular weight of mixture
$n$	Number of species in mixture
$n_p, n_n$	Number of positive (negative) ion species in mixture
$N$	Number densities
$p$	Pressure
$Pr$	(Frozen) Prandtl number (Equation 5)

$q_i$	Diffusional flux velocity of i-th species
$r$	Radial coordinate of axi-symmetric surface
$R$	Universal gas constant
$Sc$	Schmidt number
$T$	Absolute temperature
$u, v$	Parallel and normal velocities in boundary layer
$w_i$	Chemical mass generation rate of i-th species
$x, y$	Parallel and normal coordinates in boundary layer
$\alpha_i^j$	Number of atoms of element j in species i
$\beta$	Pressure gradient parameter (Equation 5)
$\xi, \eta$	Transformed parallel and normal coordinates in boundary layer (Equation 1)
$\mu$	Viscosity
$\rho$	Density

#### SUBSCRIPTS

$e$	At the outer edge of the boundary layer
$\epsilon$	Electrons
$eq$	In chemical equilibrium
$i, j, O$	Refers to species (i-th, j-th, O, etc.)
$max$	Maximum, or at maximum temperature
$w$	Wall
$\infty$	Free stream

#### SUPERSCRIPTS

$i, j, O$	Refers to element (i-th, j-th, O, etc.)
$+, -$	Charged particles

## REFERENCES

1. Blottner, F. G., "Non-Equilibrium Laminar Boundary Layer Flow of Ionized Air", AIAA Aero. Science Meeting, Jan. 1964, Preprint #64-41.
2. Blottner, F. G. and Lenard, M., "Finite Rate Plasma Generation in the Laminar Air Boundary Layer of Slender Reentry Bodies", Trans. 8th Symposium on Ballistic Missile & Space Technology, Oct. 1963, Vol II, pp. 4-33.
3. Pallone, A., J., Moore, A. J., Erdos, J. I., "Nonequilibrium Non-similar Solutions of the Laminar Boundary Layer Equations", AIAA Aero. Science Meeting, January 1964, Preprint #64-40.
4. Williams, F. A., "Production of Trace Species in Boundary Layers", AIAA Hete. Comb. Conf., December 1963, Preprint #63-506.
5. Lenard, M., "Chemically Reacting Boundary Layers", General Electric Co., Space Sciences Laboratory TIS Report R64SD14, March 1964.
6. Browne, W. G., Schwartz, E. B., "Thermo-Chemistry and Kinetics of the Cesium-Air System", General Electric Co., Internal communication 1964.
7. Bortner, M. H., "Chemical Kinetics in a Reentry Flow Field", General Electric Co., Space Sciences Laboratory, TIS Report R63SD63, August 1963.
8. Bortner, M. H., "The Chemical Kinetics of Sodium in Reentry." General Electric Co., Space Sciences Laboratory TIS Report R64SD33, April 1964.
9. Kane, J. J., "Nonequilibrium Sodium Ionization in Laminar Boundary Layers." Aerospace Corp. Rept. BSD-TDR-64-50, April 1964.

APPENDIX

CHEMICAL RATE CONSTANTS

The units are  $^{\circ}\text{K}$  (temperature), g moles/cc (concentration) and  $\text{cm}^3/\text{g mole sec}$  or  $\text{cm}^6/(\text{g mole})^2 \text{ sec}$  (rate constants for 2 and 3 body reactions respectively). Also;  $R = 1.9864 \text{ cal}/^{\circ}\text{K mole}$ .

<u>Reaction</u>	<u><math>k_{\text{FORWARD}}</math></u>	<u><math>k_{\text{REVERSE}}</math></u>
1	$2.3 \times 10^{19} T^{-1} e^{-59,400/T}$	$1.9 \times 10^{16} T^{-1/2}$
2	$8.5 \times 10^{19} T^{-1} e^{-59,400/T}$	$7.1 \times 10^{16} T^{-1/2}$
3	$3.0 \times 10^{18} T^{-1} e^{-59,400/T}$	$2.5 \times 10^{15} T^{-1/2}$
4	$3.8 \times 10^{19} T^{-1} e^{-113,200/T}$	$2 \times 10^{18} T^{-1}$
5	$1.3 \times 10^{20} T^{-1} e^{-113,200/T}$	$7 \times 10^{18} T^{-1}$
6	$1.9 \times 10^{19} T^{-1} e^{-113,200/T}$	$1 \times 10^{13} T^{-1}$
7	$2.4 \times 10^{17} T^{-1/2} e^{-75,500/T}$	$6 \times 10^{16} T^{-1/2}$
8	$6.8 \times 10^{13} e^{-37,750/T}$	$1.5 \times 10^{13}$
9	$4.3 \times 10^7 T^{3/2} e^{-19,100/T}$	$1.8 \times 10^8 T^{3/2} e^{-3020/T}$
10	$1.3 \times 10^8 T e^{-31,900/T}$	$2 \times 10^{19} T^{-1}$
11	$7.2 \times 10^8$	--
12	$8.5 \times 10^{19} T^{-.5}$	$1.4 \times 10^{12} T e^{-33800/RT}$
13	$k_{\text{reverse}} \times 7.3 \times 10^{-9} T^{1.44} e^{-10650/RT}$	--
Cesium		
14	$10^{17} T^{.07} e^{-79130/RT}$	$2 \times 10^{17}$
15	$8.7 \times 10^{16} T^{-.15} e^{-55970/RT}$	$2 \times 10^{19} T^{-.6}$
16	$1.2 \times 10^{12} T^{1.18} e^{-89730/RT}$	$3 \times 10^{19}$
17	$1.6 \times 10^{32} T^{-3.3} e^{-89780/RT}$	$4 \times 10^{39} T^{-4.5}$
18	$7.2 \times 10^{14} T^{-.67}$	--
19	$6.02 \times 10^{13} T^{-.5}$	$807 \times 10^{11} e^{-122760/RT}$
Sodium		
14	$1.8 \times 10^{15} e^{-108260/RT}$	$1.2 \times 10^{17} T^{-.5}$
15	$2.0 \times 10^{15} e^{-85415/RT}$	$1.2 \times 10^{17} T^{-.5}$

<u>Reaction</u>	<u>k<sub>FORWARD</sub></u>	<u>k<sub>REVERSE</sub></u>
16	$3.9 \times 10^6 T^{1.5} e^{-118590/RT}$	$9.8 \times 10^{14}$
17	$3.9 \times 10^{14} T^{.5} e^{-118590/RT}$	$9.8 \times 10^{22} T^{-1.0}$
18	$1.2 \times 10^{14} T^{-.75}$	--
19	$3 \times 10^{13} T^{-.5}$	$9 \times 10^{10} e^{-94753/RT}$
12 slow	$2.7 \times 10^{13} T^{.57}$	$5 \times 10^5 T^2 e^{-33800/RT}$

SPACE SCIENCES LABORATORY  
MISSILE AND SPACE DIVISION

GENERAL  ELECTRIC

TECHNICAL INFORMATION SERIES

AUTHOR M. Lenard	SUBJECT CLASSIFICATION BOUNDARY LAYER STUDIES	NO. R64SD22
		DATE August, 1964
TITLE IONIZATION OF CESIUM AND SODIUM CONTAMINATED AIR IN THE HYPERSONIC SLENDER BODY BOUNDARY LAYER		G. E. CLASS I
		GOV. CLASS None
REPRODUCIBLE COPY FILED AT MSD LIBRARY. DOCUMENTS LIBRARY UNIT. VALLEY FORGE SPACE TECHNOLOGY CENTER, KING OF PRUSSIA, PA.		NO. PAGES 30
<p>SUMMARY</p> <p>An approximate procedure is used to predict the effect on air ionization of small amounts of cesium and sodium in the ablating surface material of pointed cones. Ionization is assumed to occur due to finite rate gas phase chemical reactions in the laminar boundary layer. An 11 species (<math>N_2</math>, <math>O_2</math>, <math>N</math>, <math>O</math>, <math>NO</math>, <math>Cs</math> or <math>Na</math>, <math>NO^+</math>, <math>Cs^+</math> or <math>Na^+</math>, <math>O_2^-</math>, <math>O^-</math>, <math>e^-</math>) 16 reaction chemical system is assumed.</p>		
<p>KEY WORDS</p> <p>Seeding, slender cones, ablation</p>		

BY CUTTING OUT THIS RECTANGLE AND FOLDING ON THE CENTER LINE THE ABOVE INFORMATION CAN BE FITTED INTO A STANDARD CARD FILE

AUTHOR

*Michael Lenard*

COUNTERSIGNED

*H.G. Lew*